Proc. NIPR Symp. Upper Atmos. Phys., 9, 12-24, 1996

A CONVECTION ENHANCEMENT EVENT OBSERVED WITH THE POLAR PATROL BALLOON #4

Yusuke EBIHARA[1], Akira KADOKURA[2], Yutaka TONEGAWA[1], Fumio TOHYAMA[1], Natsuo SATO[2], Yo HIRASIMA[3], Michiyoshi NAMIKI[4], E.A. BERING III[5], J.R. BENBROOK[5] and Masaki EJIRI[2]

[1]*Tokai University, 1117 Kitakaname, Hiratsuka 259-12*
[2]*National Institute of Polar Research, 9-10, Kaga 1-chome, Itabashi-ku, Tokyo 173*
[3]*Rikkyo University, 34-1, Nishi-ikebukuro 3-chome, Toshima-ku, Tokyo 171*
[4]*The Institute of Space and Astronautical Science, 1-1, Yoshinodai 3-chome, Sagamihara 229*
[5]*Houston University, 4800 Calhourn Blvd., Houston, TX 77204-5506, U.S.A.*

Abstract: A convection enhancement event was observed with the Polar Patrol Balloon #4 which was launched at Syowa Station on December 26, 1992. This event occurred during 1700-1900 UT on December 28, 1992, when the balloon located in the afternoon sector of the sub-auroral zone. During this period, the amplitude of the southward electric field (E_S) increased from about 20 mV/m to 50 mV/m and then decreased to 20 mV/m again. The northward component of the magnetic field variation (B_H) also increased from 200 nT to 600 nT, and then decreased to about 100 nT. The maximum time of E_S lagged about 12 min after the B_H maximum time (t_{Bmax}). We could estimate the height integrated ionospheric electric conductivity from these horizontal electric field and magnetic field data. Before t_{Bmax} Hall conductivity (σ_H) was about two times greater than Pedersen conductivity (σ_P), and after t_{Bmax} σ_H decreased monotonously to become smaller than σ_P, while σ_P maintained a nearly constant value. Around t_{Bmax} both σ_H and σ_P were enhanced by about 1.5 times in about 10 min, and energetic particle precipitation was observed with the on-board X-ray counter. We could summarize this event as follows: there was stable enough particle precipitation to maintain σ_H before t_{Bmax}: As E_S increased, the ionospheric Hall current increased, and B_H increased. Around t_{Bmax} a large quantity of particles precipitated above the balloon, ionospheric conductivities and Hall current reached a maximum value, and thus the B_H reached a maximum value. After t_{Bmax} σ_H and B_H decreased because the energy spectrum of the precipitation became softer, while E_S continued to increase. E_S reached a maximum value about 12 min after t_{Bmax}.

From the ground-based data in the southern and northern hemispheres and also satellite IMF data, it was concluded that this event was not an isolated disturbace confined just around the balloon location, but was a global feature of the ionospheric convection variation corresponding to the IMF fluctuation.

1. Introduction

Three Polar Patrol Balloon (PPB) experiments (PPB#4, #5, and #6) were carried out

by the 34th Japanese Antarctic Research Expedition (JARE-34) at Syowa Station in Antarctica from December 1992 to January 1993. The scientific purposes of these experiments have been described by TOHYAMA *et al.* (1992), KADOKURA *et al.* (1992), and MURAKAMI *et al.* (1992). The launching procedure and balloon trajectories have been described by NAMIKI *et al.* (1993), and preliminary observation results have been described by EJIRI *et al.* (1995), TOHYAMA *et al.* (1993a), SUZUKI *et al.* (1993), and KUNIMOTO *et al.* (1993). In this paper, we will report an interesting event observed with PPB#4. Payload configurations of PPB#4 and #5 were the same and the installed instruments were a tri-axial fluxgate magnetometer, proton magnetometer, three axis electric field detectors, and auroral X-ray counter to study atmospheric and space electro-magnetic dynamics. Many observations using this kind of instrument with stratospheric balloon were started by MOZER and SERLIN (1969). Long duration observation using a superpressure balloon was also reported by DOWDEN (1993). The unique point of our PPB#4 and #5 as compared with these previous works was the balloon attitude determination system using two sun sensors and two clinometers, and we can calculate the magnetic field observed on PPB on the basis of earth-fixed coordinates. In the following sections, we will describe the instrumentation of PPB#4 in some detail (Section 2), and show observation results concerning interesting events. We also show the ground-based and satellite data at that time (Section 3), and summarize the characteristics of the event (Section 4).

2. Instrumentation of PPB#4

Observation data were obtained with the ARGOS data acquisition system. In order to increase data transmission rate, 41 IDs are assigned on one ARGOS transmitter, which is called the "Multi-ID ARGOS system" (FUJII *et al.*, 1992). One hour data are stored in an on-board memory, and transmitted repeatedly six times in the next 1 hour. One ARGOS frame consists of 32 words (1 byte/word), and the frame sampling rate is 30 s/frame. In one frame, there are fluxgate magnetometer data (6 words), proton magnetometer (2 words), electric field (7 words), and X-ray counter (8 words). Fluxgate magnetometer data are sampled at the time when sunlight enters either the A or B sun-sensor. At the same time, the two-axis clinometer data are also sampled, they occupy 4 words in the telemetry frame. The field of view of each sun-sensor is very narrow in azimuth and wide in elevation, and the two sensors are placed so as to look in opposite directions. The planned spin rate of the gondola is 1 rpm, so fluxgate magnetometer data are renewed about every 30 s. Using the clinometer data with the sun-sensor information, the temporal and spatial variations of the gondola can be calculated assuming that the centrifugal force due to pendulum motion of the gondola should be negligibly small. The resolution of this attitude determination is estimated to be 0.01°. If the gondola attitude is determined, we can calculate the magnetic field vector in the earth-fixed frame through a coordinate transfer, and then calculate the variation from the quiet time IGRF model value. Resolution of the measured value is 1 nT. Proton magnetometer data are used for an anomaly survey as done in the previous work (TOHYAMA *et al.*, 1993b) and also for calibrating the fluxgate magnetometer data.

Vector electric field is measured with an ordinary three axis double probe system. Phase angle and amplitude of the horizontal component and the intensity of the vertical

component are calculated by an on-board CPU at every 30 s with the help of the fluxgate magnetometer horizontal outputs. Resolution of the horizontal measurement is 0.86 mV/m for the amplitude and 1.5° for phase angle, and 13 mV/m for vertical measurement. Gondola spin rate is also calculated by the same CPU; its resolution is 0.5 s.

The X-ray counter has a field of view of 90° and four discrete levels, 30–50, 50–70, 70–90, and 90–120 keV. The dynamic range of the measurement is 0–219, and accumulated count for 15 s is put on each telemetry word.

3. Convection Enhancement Event

3.1. Balloon observation

PPB#4 was launched at Syowa Station at 1324 UT on December 26, 1992. After launch, the balloon drifted westward and in the lower magnetic latitude direction, The event mentioned in Section 1 was observed during 1700–1900 UT on December 28, 1992 when the balloon was located near the lower latitude side of Sanae Station. Figure 1 shows the trajectory and the location of the balloon in this observation. The balloon was located in the sub-auroral zone (invariant latitude of 56.9–56.5°) and in the afternoon sector (MLT of 1504–1655) during this event.

A summary plot of the data observed on December 28, 1992 is shown in Fig. 2. There are several gaps in the data during one hour (*e.g.* 0200–0300 UT), which means that

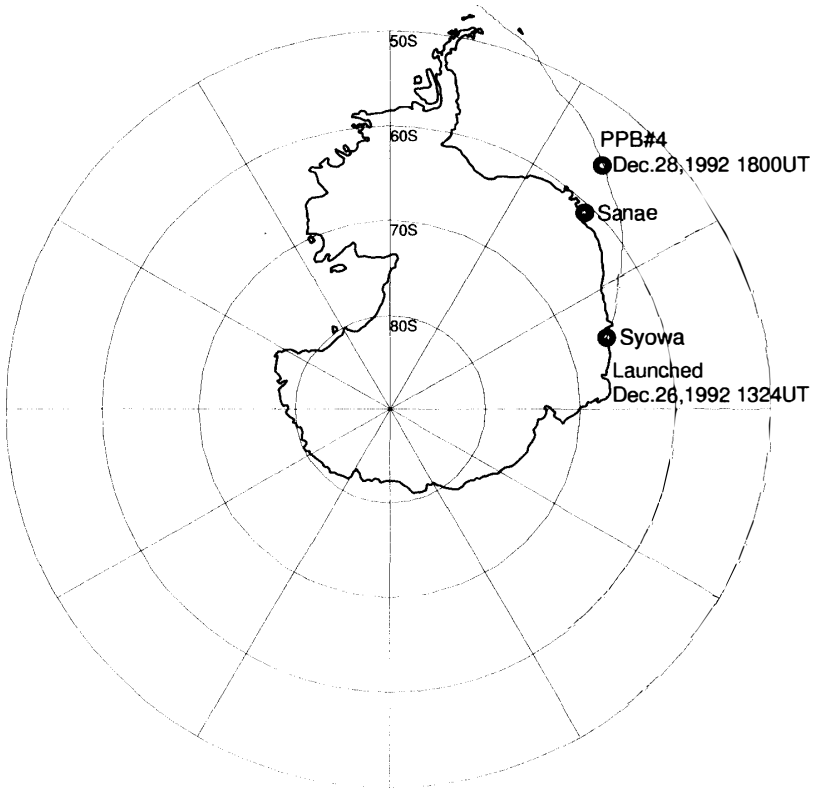

Fig. 1. Trajectory of the PPB#4 in invariant latitude vs. magnetic longitude coordinate. Balloon location at 1800 UT on December 28, 1992 is shown by a circle on the trajectory.

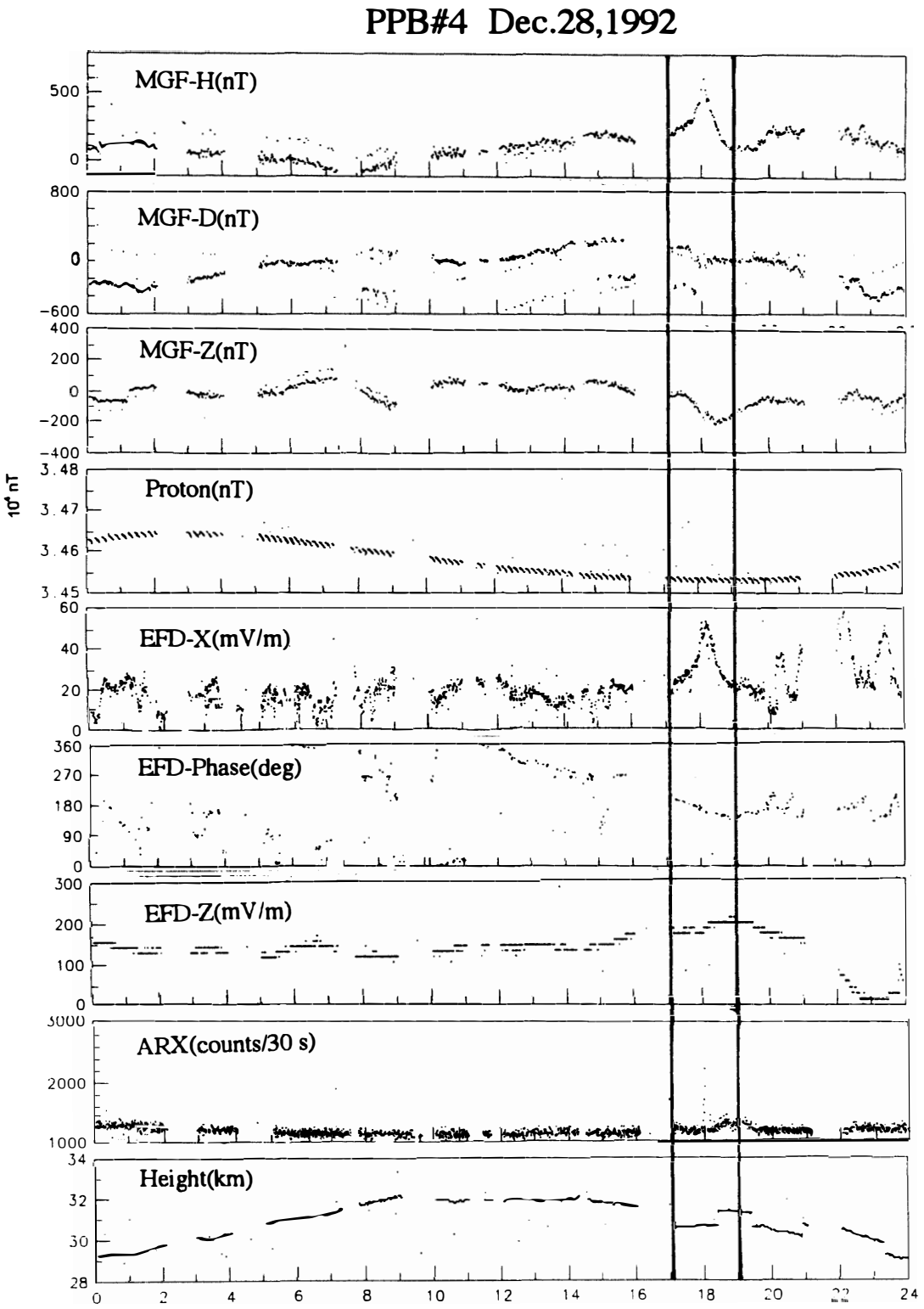

Fig. 2. A summary plot of the PPB#4 data obtained on December 28, 1992. Each panel from the top shows H-, D-, and Z-components of the magnetic field, magnetic total intensity observed with the proton magnetometer, amplitude and phase angle from magnetic north of the horizontal electric field, intensity of the vertical electric field, accumulated total count of the auroral X-ray counter, and balloon altitude.

the balloon could not encounter with ARGOS satellites for one hour. The top three panels show the magnetic field variation from IGRF-90 model for the geomagnetic north- (MGF-H), east- (MGF-D), and downward (MGF-Z) components. Though two separated data sequences can be seen in these panels, which is caused by ambiguity in the alignment of the two-axis clinometer, we can determine which data are correct. In the electric field panels, horizontal electric field amplitude (EFD-Amp) and eastward phase angle from magnetic north (EFD-Phase), and downward electric field intensity (EFD-Z) are shown. On this day, the vertical electric field was downward, which was characteristic under fair weather conditions. The observed horizontal electric field seems to be mainly of ionospheric origin because the balloon altitude was maintained above a sufficient level for ionospheric observation, as can be seen in the bottom panel.

During 1700–1900 UT, a remarkable variation can be seen in the MGF-H and EFD-Amp panels. Each value gradually increased from 1700 UT, reached a maximum around 1800 UT, and then gradually decreased until 1900 UT. The maximum time of EFD-Amp shows a small time-lag from the variaton of MGF-H. Variation amplitude was about 30 mV/m for EFD-Amp and about 400 nT for MGF-H. From the EFD-Phase panel, it can be seen that the horizontal electric field was almost directed southward (poleward) during this period. The auroral X-ray panel shows a spike-like increase of the count rate around 1800 UT.

Height integrated ionospheric electric conductivity can be estimated using the horizontal electric field and magnetic field data by the following relation:

$$\begin{pmatrix} j_X \\ j_Y \end{pmatrix} = \begin{pmatrix} \sigma_{XX} & \sigma_{XY} \\ -\sigma_{XY} & \sigma_{YY} \end{pmatrix} \begin{pmatrix} E_X \\ E_Y \end{pmatrix}, \tag{1}$$

$$\sigma_{XX} \simeq \frac{\sigma_1}{\sin^2 I}$$

$$\sigma_{YY} \simeq \sigma_1$$

$$\sigma_{XY} \simeq \frac{\sigma_2}{\sin I}$$

where suffixes X and Y show the southward and eastward components, respectively. E_X and E_Y are the observed horizontal electric field amplitudes, assuming that they are of purely ionospheric origin. j_X and j_Y are the equivalent current intensities calculated from the magnetic field variation. I is inclination of the magnetic field at the ionosphere level, and σ_P and σ_H are height integrated Pedersen and Hall conductivities, respectively.

Figure 3 shows the time-expanded plot of the observation data during 1700–2000 UT with the conductivity (top panel) and IMF-B_Z component (bottom panel) plots. The magnitude of the horizontal magnetic field reached a maximum at 1800 UT, and the horizontal electric field reached a maximum at 1812 UT. Hence the time lag between them was about 12 min. During an about 10-min interval around 1800 UT, the X-ray count increased to the maximum value of 2900 counts/30 s from its background level of 1300 counts/30 s. Corresponding to the X-ray count enhancement, conductivities, σ_P and σ_H, also increased to their maximum values of about 10 mho and 16 mho, respectively, around 1800 UT. Before 1800 UT, σ_H was about two times greater than σ_P, and after 1800 UT σ_H decreased monotonically to become smaller than σ_P, while σ_P maintained nearly

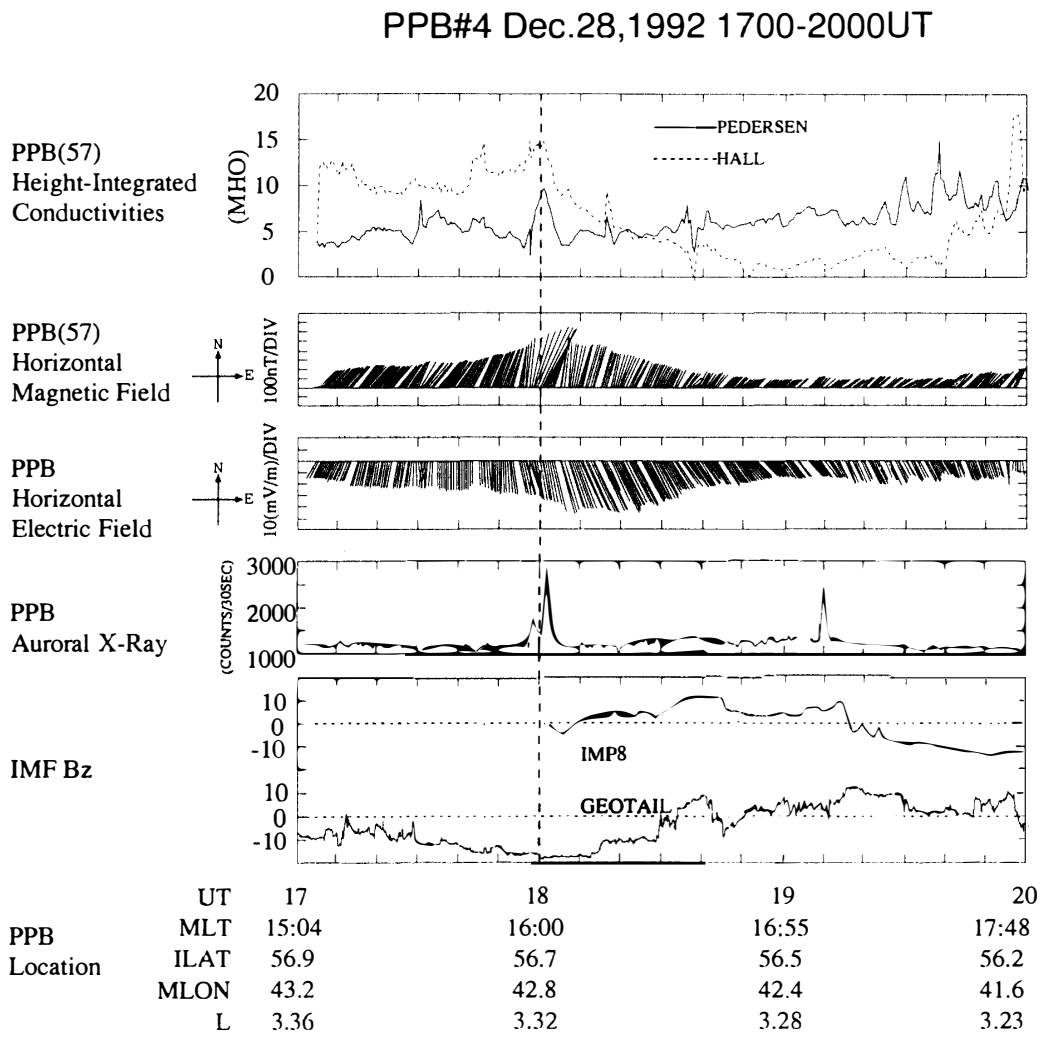

Fig. 3. Each panel from the top shows the ionospheric height integrated Pedersen and Hall conductivities calculated using eq. (1), horizontal vector of the observed magnetic field variation, horizontal vector of electric field, X-ray count, and IMF-B_Z data from IMP-8 and GEOTAIL satellites.

constant value during whole period. It is known that the peak altitude of the Pedersen conductivity is higher than that of the Hall conductivity, so this variation of the ratio between σ_P and σ_H implies that the altitude of the effective current layer becomes high after 1800 UT. The energy spectrum of precipitating particles responsible for creating the conductivity became soft in this time. Before 1800 UT a rather stable harder precipitation continued at least for about one hour and σ_H maintained about 10 mho.

As the southward (poleward) electric field gradually increased, westward (sunward) ionospheric convection increased and thus the northward magnetic variation at the balloon altitude increased. Around 1800 UT, particle precipitation flux became a maximum; it created the maximum ionospheric conductivities and the magnetic variation. After 1800 UT, the magnetic variation mainly decreased because the ionospheric Hall conductivity decreased, while the electric field amplitude continued to increase to become a maximum at 1812 UT. If this electric field variation was assumed to be of magnetospheric origin and

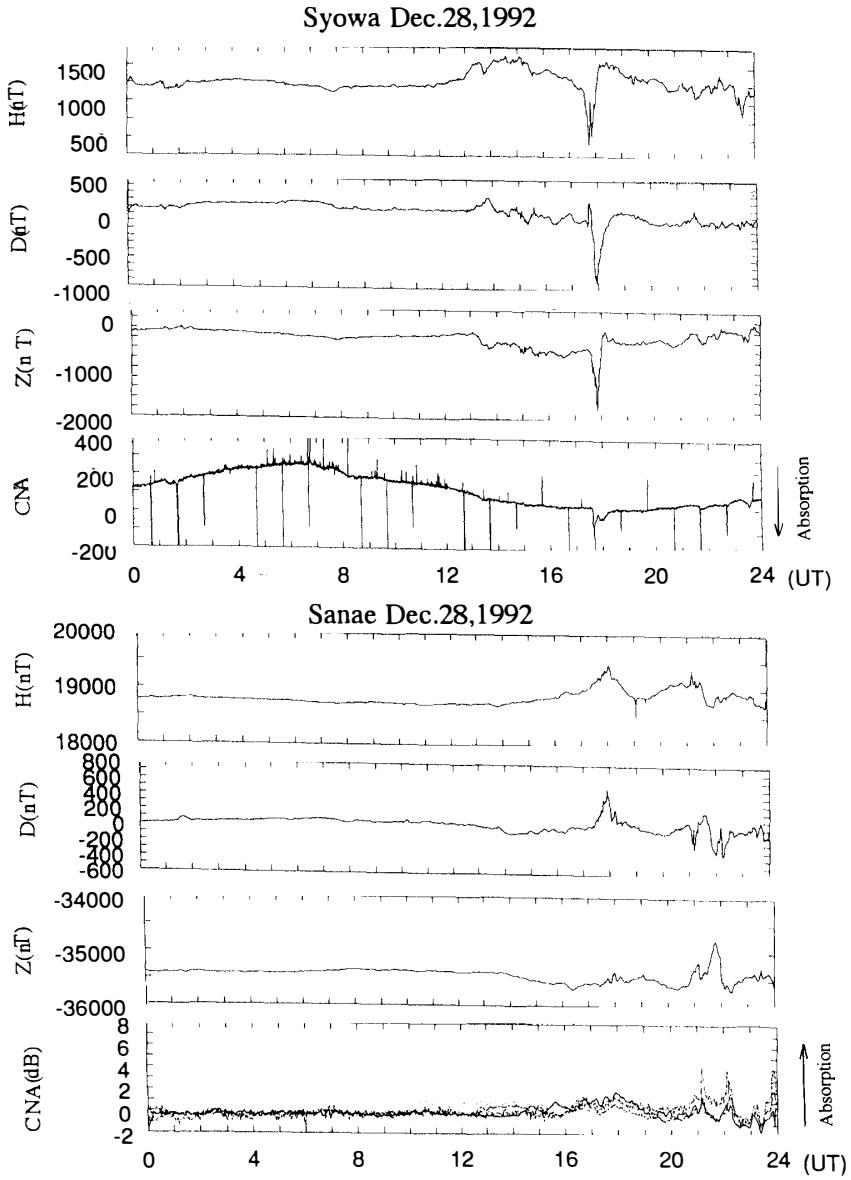

Fig. 4. A daily plot of magnetometer and riometer data obtained at Syowa Station (upper panels) and Sanae Station (lower panel) on December 28, 1992. The two vertical lines show the event period.

we project it onto the magnetospheric equatorial plane, the observed southward variation corresponds to the dawn-to-dusk electric field variation in the magnetosphere. From many previous works, this dawn-to-dusk electric field depends on the north-south (Z-) component of the IMF (IMF-B_Z). If IMF-B_Z increases in negative value, the dawn-to-dusk electric field increases, and *vice versa*. The bottom panel of Fig. 3 shows the key-parameter data of the IMF-B_Z obtained by IMP-8 and GEOTAIL satellites. At this time, IMP-8 was located at around (2.3, −30.7, −2.7) in earth radii in GSM (X, Y, Z) coordinates, and GEOTAIL was located at (−146, −43, −8). IMP-8 is thought to be in the solar wind regime, and GEOTAIL is in the magneto-sheath region in the far tail. GEOTAIL data lagged about 40 min from IMP-8 data. Because there is a data gap in the

IMP-8 data between 1700–1802 UT, we substitute the 40-min advanced GEOTAIL data, which are shown with a dashed line. It can be seen that IMF-B_Z decreased to a large negative minimum value of -18 nT around 1800 UT, almost corresponding to the enhancement of electric field by balloon observation. Though it is difficult to determine the precise response time between southward IMF variations and electric field enhancement, it may be said that observed electric field variation was caused by the IMF-B_Z variation.

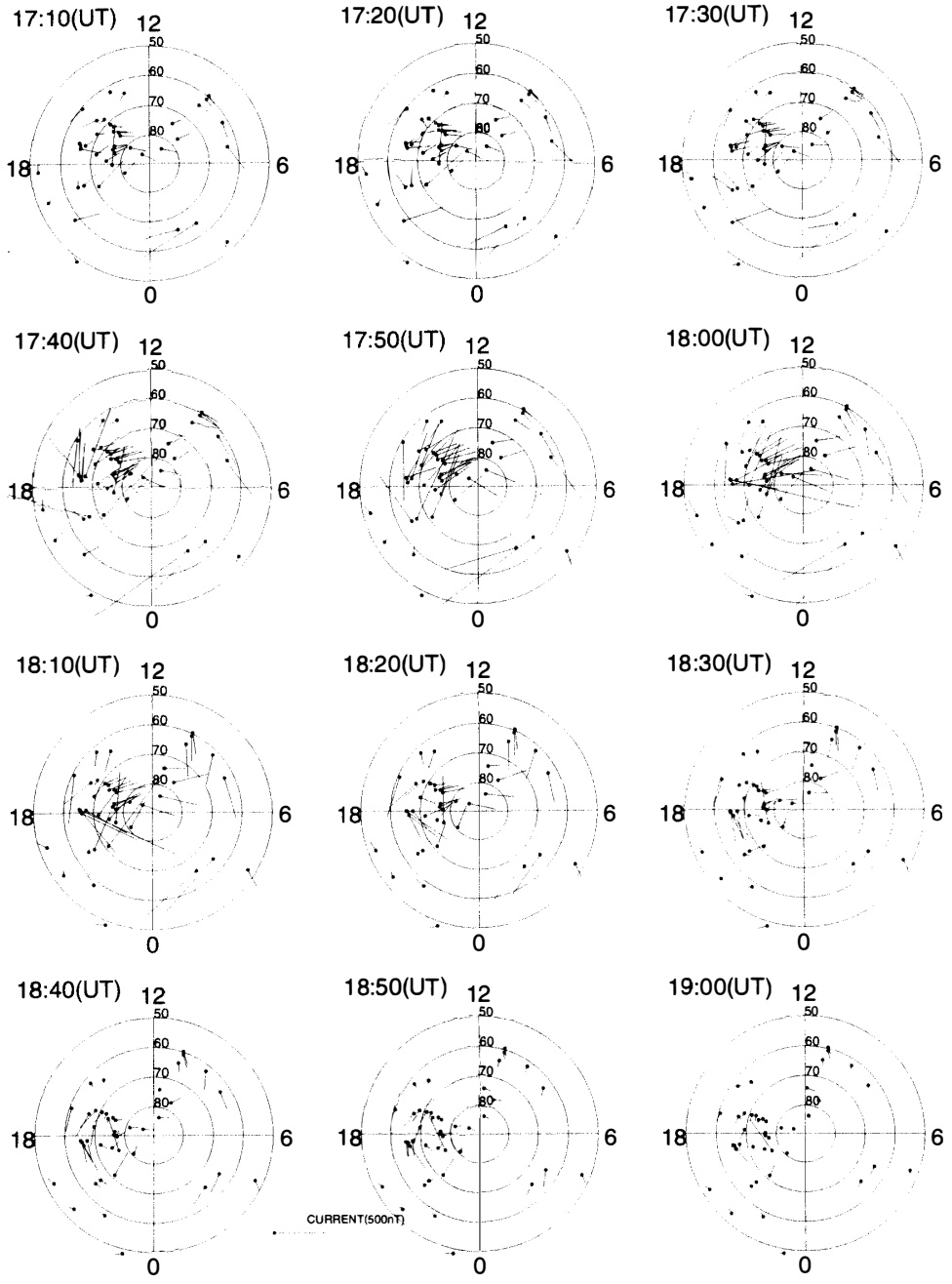

Fig. 5. Development of the equivalent current distribution in the northern hemisphere in the inveriant latitude vs. MLT coordinate during 1700–1850 UT on December 28, 1992.

3.2. Ground-based data

In order to check whether this event was a world-wide phenomenon or not, we looked at ground-based data obtained at 41 observatories around the world.

Figure 4 shows magnetometer and riometer data obtained at two southern hemisphere stations, Syowa (upper panels) and Sanae (lower panels), on the same day. According to Sanae Station's magnetogram, the H-component of the magnetic field shows a similar variation to the PPB data observed near Sanae, but the variation amplitude is about 700 nT, which is larger than the PPB value. The variation of the *D*-component was not so remarkable as PPB data, but the magnitude of the *D*-component at Sanae was comparable to that of the *H*-component. At Syowa Station in the auroral zone, variation features were different from those of sub-auroral zone data. Each magnetic field component shows a sharp negative variation of amplitude about 1000 nT, and the riometer data show that energetic particle precipitation occurred suddenly. All these features indicate that a sub-storm should occur during this period. From the 210° magnetic meridian chain data, Pi2 events, which are good indicators of sub-storm onset, were observed at 1707 and 1738 UT (YUMOTO, K., private communication, 1994).

Figure 5 shows the development of the equivalent current distribution during 1700–1850 UT in the invariant latitude *vs.* MLT coordinates, which is calculated from the magnetometer data at the 41 observatories. Locations of the southern hemispheric

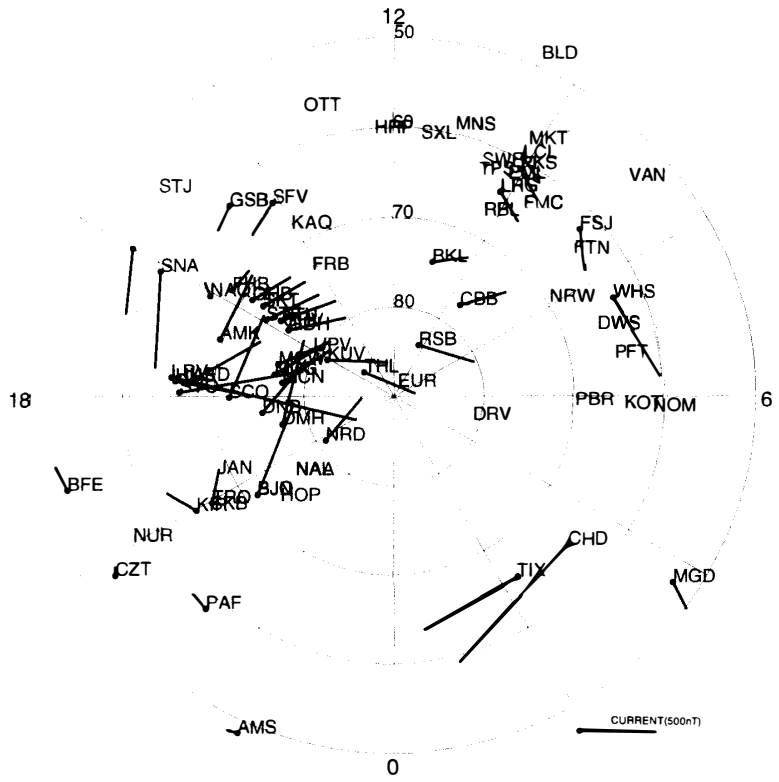

Fig. 6. An equivalent current distribution in the northern hemisphere in the invariant latitude vs. MLT coordinate at 1800 UT on December 28, 1992 when the current intensity reached the maximum. The thin line shows the PPB trajectory projected on the northern hemisphere map.

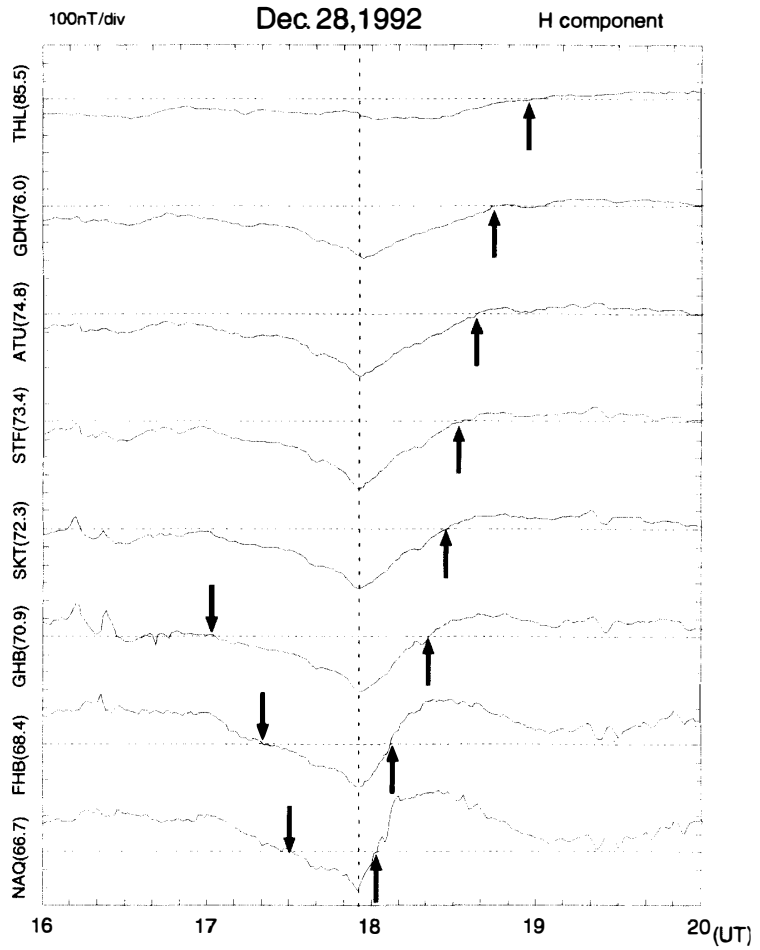

Fig. 7. Magnetic H-component variations at the westside Greenland magnetometer chain stations. Each arrow shows current reversal time.

observatories are projected on the northern hemispheric map using IGRF-90 and Tsyganenko-87 geomagnetic field models. It can be seen that during this period ionospheric current intensity was gradually enhanced to become a maximum around 1800 UT and then weakened. This variation occurred world-wide. A snapshot of the current pattern at 1800 UT is shown in Fig. 6 with a northern hemispheric map. The current pattern is basically consistent with the HEPPNER and MAYNARD (1987) result for the similar IMF-$B_Y > 0$ and $-B_Z < 0$ case.

Figure 7 shows the variation of the magnetic H-component observed at eight observatories of the west Greenland magnetometer chain which is located along almost the same magnetic meridian as Sanae and PPB, during this event. Thick black arrows in Fig. 6 indicate the time when the ionospheric current direction was reversed from eastward to westward (downward arrows) and from westward to eastward (upward ones). A break line indicates the westward current maximum time, at 1754 UT. Before the maximum time the current reversal position moved to lower latitudes with the moving speed of 15 km/min, and after that, it moved back to higher latitudes with the speed of 22 km/min. These movements imply that the polar cap region was gradually expanding before 1754 UT, and

then gradually shrinking, which seems to relate to the IMF-B_Z variation mentioned in Section 3.1.

All the ground-based data mentioned above show that this event was not confined just around the balloon location, but a global feature of ionospheric current variation phenomenon related to the IMF-B_Z variation.

4. Summary

A convection enhancement event was observed with the instruments aboard the PPB#4 when the balloon was located in the afternoon sector of the sub-auroral zone. The amplitude of the southward electric field (E_S) increased by about 2.5 times, and the northward component of the magnetic field variation (B_H) also increased by about 3 times. The electric field maximum time lagged about 12 min after the magnetic field maximum time (t_{Bmax}). We estimated the height integrated ionospheric electric conductivity from these horizontal electric field and magnetic field data. Before t_{Bmax} Hall conductivity (σ_H) was about two times greater than Pedersen conductivity (σ_P), and after t_{Bmax} σ_H decreased monotonically to become smaller than σ_P, while σ_P maintained a nearly constant value. Around t_{Bmax} both σ_H and σ_P were enhanced about 1.5 times during the interval of 10 min, and energetic particle precipitation was observed by the on-board X-ray counter. We can summarize this event as follows: there was stable enough harder particle precipitation to maintain σ_H before t_{Bmax}: As E_S increased, ionospheric Hall current increased and then B_H increased. Around t_{Bmax} there was a large amount of particle precipitation above the balloon. Therefore ionospheric conductivities and Hall current reached a maximum value, and B_H reached a maximum value. After t_{Bmax} σ_H decreased because the energy spectrum of the precipitation became softer, and B_H decreased. On the other hand, E_S continued to increase, and reached a maximum value about 12 min after t_{Bmax}.

During this event IMF-B_Z decreased to a large negative value and then increased to become positive. The E_S variation may be related to this IMF-B_Z variation.

The magnetic H-component at Sanae Station close to the balloon location showed similar variation to the balloon data, while the magnetometer and riometer data at Syowa Station on the evening side of the auroral zone showed a sub-storm-like variation.

Global equivalent current distribution was calculated from the ground-based magnetometer data at many observatories in the southern and northern hemispheres. It was found that ionospheric current intensity was enhanced world-wide during this event. Magnetic H-component variation at the west Greenland magnetometer chain stations suggested that the polar cap region was gradually expanding and then gradually shrinking during this event.

From these ground-based data, it is concluded that this event was not an isolated disturbance confined just around the balloon location, but was a global feature of ionospheric current variation corresponding to the IMF variation.

The derivation of the magnetic vector variation by using an attitude determination system and the on-board data processing of electric field were newly attempted in the PPB #4. From the comparision between balloon and ground data, it can be said that those new attempts were very successful for this observation and applicable to other balloon experiments for studying the atmospheric and space electro-magnetic dynamics.

Acknowledgments

We wish to express our sincere thanks to all members of JARE-34 who carried out PPB#4 PPB#5, and PPB#6 experiments. Thanks are due to Prof. T. SAKURAI (Tokai University) for his many helpful comments. The Greenland magnetometer data and the Sanae data are kindly supplied from Dr. E.F. CHRISTENSEN at DMI, and Mr. M.J. MATHEWS in SANAP, respectively. We wish to thank Dr. T. IYEMORI and all staff of WDC-C2 for Geomagnetism in Kyoto University for providing some magnetograms. We also would like to thank Dr. K. HAYASHI for providing some magnetograms from the STEP Polar Network. This PPB project have been done under the PPB Working Group. We are very grateful to all members of the Working Group. The data processing has been carried out at the Computer Center of Tokai University and the Information Science Center of the National Institute of Polar Research.

References

DOWDEN, R.L. (1993): Extended life balloon-borne observatories. STEP Int., **3**(6), 1–5.

EJIRI, M., AKIYAMA, H., BERING, E.A., FUJII, R., HAYASHI, M., HIRASIMA, Y., KADOKURA, A., KANZAWA, H., KODAMA, M., MIYAOKA, H., MURAKAMI, H., NAKAGAWA, M., NAMIKI, M., NISHIMURA, J., OHTA, S., SUZUKI, H., TOHYAMA, F., TONEGAWA, Y., YAJIMA, N., YAMAGAMI, T., YAMAGISHI, H. and YAMANAKA, M.D. (1995): Experimental results of Polar Patrol Balloon project in Antarctica. Proc. NIPR Symp. Upper Atmos. Phys., **8**, 60–64.

FUJII, R., ONO, K. and OHTA, S. (1992): Data transfer system using a multi-ID ARGOS transmitter for the Antarctic Polar Patrol Balloon experiment. Nankyoku Shiryô (Antarct. Rec.), **36**, 350–362 (in Japanese with English abstract).

HEPPNER, J.P. and MAYNARD, N.C. (1987): Empirical high-latitude electric field models. J. Geophys. Res., **92**, 4467–4489.

KADOKURA, A., EJIRI, M., BERING, E.A., BENBROOK, J.R., FUJII, R. and TONEGAWA, Y. (1992): Ionospheric electric field observation plan with JARE-34 PPB. Dai-Kikyu Shinpojiumu (Proc. Balloon Symp. at ISAS in 1992). Sagamihara, Inst. Space Astronaut. Sci., 221–226 (in Japanese).

KUNIMOTO, S., MURAKAMI, S., NAKAGAWA, M., TAKAHASHI, T., NISHIMURA, J., OHTA, S., NAMIKI, M., YAMAGAMI, T., KODAMA, M., KOHNO, T., YAMAUCHI, M., YAMAGIWA, I., HIRASIMA, Y., MORIMOTO, K., MURAKAMI, H. and SUZUKI, H. (1993): Cosmic ray observation with PPB#6. Dai-Kikyu Shinpojiumu (Proc. Balloon Symp. at ISAS in 1993). Sagamihara, Inst. Space Astronaut. Sci., 45–48 (in Japanese).

MOZER, F.S. and SERLIN, R. (1969): Magnetospheric electric field measurements with balloons. J. Geophys. Res., **74,** 4739–4754.

MURAKAMI, S., NAKAGAWA, M., TAKAGI, H., TAKAHASHI, Y., NISHIMURA, J., YAMAGAMI, T., KODAMA, M., KOHNO, T., YAMAUCHI, M., HIRASIMA, Y., MURAKAMI, H., MORIMOTO, K. and YAMAGIWA, I. (1992): Cosmic ray observaion plan with PPB#6. Dai-Kikyu Shinpojiumu (Proc. Balloon Symp. at ISAS in 1992). Sagamihara, Inst. Space Astronaut. Sci., 227–232 (in Japanese).

NAMIKI, M., TONEGAWA, Y., SATO, N. and PPB working group (1993): Launching operation of the Polar Patrol Balloon experiment in 1992. Dai-Kikyu Shinpojiumu (Proc. Balloon Symp. at ISAS in 1993). Sagamihara, Inst. Space Astronaut. Sci., 33–36 (in Japanese).

SUZUKI, H., HIRASIMA, Y., MURAKAMI, H., SIMOBAYASHI, N., YAMAGAMI, T., NAMIKI, M., TONEGAWA, Y., EJIRI, M., SATO, N., NAKAGAWA, M., NISHIMURA, J., KODAMA, M. and PPB working group (1993): X-ray observation results with Polar Patrol Balloon (PPB). Dai-Kikyu Shinpojiumu (Proc. Balloon Symp. at ISAS in 1993). Sagamihara, Inst. Space Astronaut. Sci., 41–44 (in Japanese).

TOHYAMA, F., FUJII, R., EJIRI, M. and YAJIMA, N. (1993): Observations of the geomagnetic field by Polar Patrol Balloon (PPB) experiment in Antarctica. Proc. NIPR Symp. Upper Atmos. Phys., **6**, 15–24.

TOHYAMA, F., TONEGAWA, Y., KADOKURA, A., EJIRI, M., SATO, N., YAJIMA, N., NAMIKI, M., MATSUHASHI, N., EBIHARA, Y. and PPB working group (1993b): Balloon observation of magnetic field in Antarctica. Dai-Kikyu Shinpojiumu (Proc. Balloon Symp. at ISAS in 1993). Sagamihara, Inst. Space Astronaut. Sci., 37–40 (in Japanese).

TOHYAMA, F., TONEGAWA, Y., SATO, N., KADOKURA, A., EJIRI, M., NAMIKI, M., YAJIMA, N. and PPB working group (1992): Vector measurement plan of magnetic field with Polar Patrol Balloon (PPB). Dai-Kikyu Shinpojiumu (Proc. Balloon Symp. at ISAS in 1992). Sagamihara, Inst. Space Astronaut. Sci., 215–220 (in Japanese).

YUMOTO, K., TANAKA, Y., OGUTI, T., SHIOKAWA, K., YOSHIMURA, Y., ISONO, A., FRASER, B.J., MENK, F.W., LYNN, J.W., SETO, M. and 210° MM Magnetic Observation Group (1992): Globally coordinated magnetic observations along 210° magnetic meridian during STEP period: 1. Preliminary results of low-latitude Pc 3's. J. Geomagn. Geoelectr., **44**, 261–276.

(Received September 14, 1995; Revised manuscript accepted September 18, 1995)